7 Speckle Metrology

7.1 Electronic Speckle Pattern Interferometry (ESPI)

Electronic Speckle Pattern Interferometry (ESPI) is a method, similar HI, to measure optical path changes caused by deformation of opaque bodies or refractive index variations within transparent media [48, 94]. In ESPI electronic devices (CCD's) are used to record the information. The speckle patterns which are recorded by an ESPI system can be considered as image plane holograms. Image plane holograms are holograms of focussed images. Due to the digital recording and processing, ESPI is designated also as *Digital Speckle Pattern Interferometry* (DSPI). Another designation is *TV-holography*. However, instead of hologram reconstruction the speckle pattern are correlated.

The principal set-up of an Electronic Speckle Pattern Interferometer is shown in figure 7.1. The object is imaged onto a camera (CCD) by a lens system. Due to the coherent illumination the image is a speckle pattern. According to Eq. (2.57) the speckle size depends on the wavelength, the image distance and the aperture diameter. The speckle size should match with the resolution (pixel size) of the electronic target. This can be achieved by closing the aperture of the imaging system.

The speckle pattern of the object surface is superimposed on the target with a spherical reference wave. The source point of the reference wave should be located in the centre of the imaging lens. Due to this in-line configuration the spatial frequencies are resolvable by the CCD. In practice the reference wave is coupled into the set-up by a beam splitter (as shown in figure 7.1) or guided via an optical fibre, which is mounted directly in the aperture of the lens system.

The intensity on the target is:

$$\begin{aligned} I_A(x,y) &= \left| a_R(x,y)\exp(i\varphi_R) + a_O(x,y)\exp(i\varphi_O) \right|^2 \\ &= {a_R}^2 + {a_O}^2 + 2a_R a_O \cos(\varphi_O - \varphi_R) \end{aligned} \tag{7.1}$$

$a_R \exp(i\varphi_R)$ is the complex amplitude of the reference wave and $a_O \exp(i\varphi_O)$ is the complex amplitude of the object wave in the image plane. The term $(\varphi_O - \varphi_R)$ is the phase difference between reference and object wave, which varies randomly from point to point. This speckle interferogram is recorded and electronically stored.

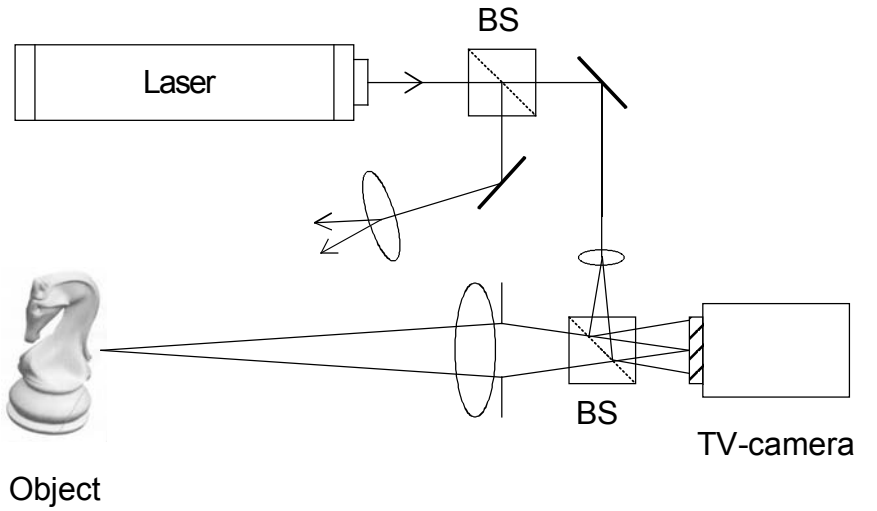

Fig. 7.1. Electronic Speckle Pattern Interferometer

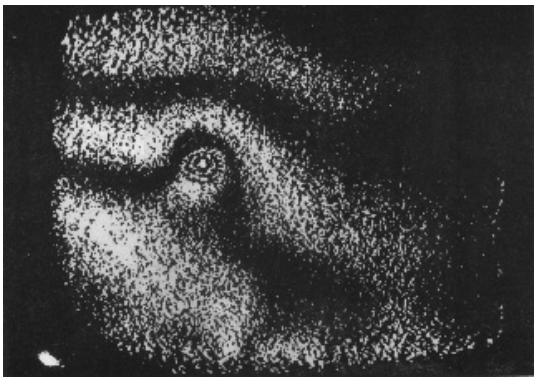

Fig. 7.2. ESPI image

The set-up in figure 7.1 is sensitive to out-of-plane deformations, i. e. deformations perpendicular to the object surface. A displacement of d_z corresponds to a phase shift of

$$\Delta\varphi = \frac{4\pi}{\lambda} d_z \tag{7.2}$$

After deformation a second speckle pattern is recorded:

$$I_B(x,y) = \left|a_R(x,y)\exp(i\varphi_R) + a_O(x,y)\exp(i\varphi_O + \Delta\varphi)\right|^2 \qquad (7.3)$$
$$= a_R{}^2 + a_O{}^2 + 2a_R a_O \cos(\varphi_O - \varphi_R + \Delta\varphi)$$

These two speckle pattern are now subtracted:

$$\Delta I = \left|I_A - I_B\right| = \left|2a_R a_O\left(\cos(\varphi_O - \varphi_R) - \cos(\varphi_O - \varphi_R + \Delta\varphi)\right)\right| \qquad (7.4)$$
$$= 2a_R a_O\left|\sin\left(\varphi_0 - \varphi_R + \frac{\Delta\varphi}{2}\right)\sin\frac{\Delta\varphi}{2}\right|$$

The intensity of this difference image is minimal at those positions, where $\Delta\varphi = 0,2\pi,\ldots$. The intensity reaches its maximum at those positions, where $\Delta\varphi = \pi,3\pi,\ldots$. The result is a pattern of dark and bright fringes, similar to a holographic interferogram. However, differences to HI are the speckle appearance of the fringes and the loss of the three-dimensional information in the correlation process. A typical ESPI subtraction pattern is shown in figure 7.2.

As already mentioned, the set-up of figure 7.1 is only sensitive to out-of plane motions. In-plane displacements can be measured with the set-up of figure 7.3. Two plane waves illuminate the object symmetrically at the angles $\pm\theta$ to the z-axis. The object is imaged by a camera. Again the speckle size is adapted to the target resolution by the aperture of the imaging system. The phase change due to an in-plane displacement can be derived by geometrical considerations, similar to the HI displacement calculations. The phase change of the upper beam is

$$\Delta\varphi_1 = \frac{2\pi}{\lambda}\vec{d}\left(\vec{b} - \vec{s}_1\right) \qquad (7.5)$$

with displacement vector $\vec{d}$. The unit vectors $\vec{b}$, $\vec{s}_1$ and $\vec{s}_2$ are defined in figure 7.3. The corresponding phase shift of the lower beam is

$$\Delta\varphi_2 = \frac{2\pi}{\lambda}\vec{d}\left(\vec{b} - \vec{s}_2\right) \qquad (7.6)$$

The total phase shift is

$$\Delta\varphi = \Delta\varphi_1 - \Delta\varphi_1 = \frac{2\pi}{\lambda}\vec{d}\left(\vec{s}_2 - \vec{s}_1\right) \qquad (7.7)$$

The vector $\left(\vec{s}_2 - \vec{s}_1\right)$ is parallel to the x-axis, its length is $2\sin\theta$. The result for the total phase shift as measured by the camera is therefore:

$$\Delta\varphi = \frac{4\pi}{\lambda}d_x \sin\theta \qquad (7.8)$$

By using non-symmetrical illumination, the method also becomes sensitive to out-of-plane displacements.

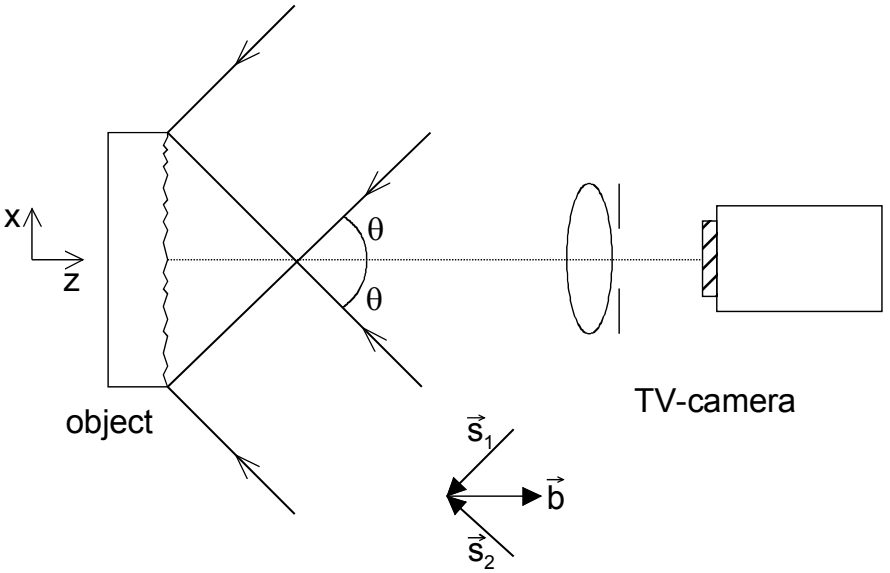

Fig. 7.3 In-plane sensitive speckle interferometer

As for HI the phase cannot be determined from a single speckle pattern. The interference phase has to be recovered e. g. with phase shifting methods [19, 152, 153]. Phase shifting ESPI requires to record at least 3 speckle interferograms with mutual phase shifts *in each state*. Any of the various phase shifting methods can be applied. Here the algorithm with 4 recordings and unknown, but constant phase shift angle α is used. The equation system for the initial state is:

$$\begin{aligned} I_{A,1} &= a_R{}^2 + a_O{}^2 + 2a_R a_O \cos(\varphi_0 - \varphi_R) \\ I_{A,2} &= a_R{}^2 + a_O{}^2 + 2a_R a_O \cos(\varphi_0 - \varphi_R + \alpha) \\ I_{A,3} &= a_R{}^2 + a_O{}^2 + 2a_R a_O \cos(\varphi_0 - \varphi_R + 2\alpha) \\ I_{A,4} &= a_R{}^2 + a_O{}^2 + 2a_R a_O \cos(\varphi_0 - \varphi_R + 3\alpha) \end{aligned} \tag{7.9}$$

The dependence of the intensities and amplitudes from the spatial coordinates *(x,y)* has been omitted. This equation system has following solution:

$$\varphi_O - \varphi_R = \arctan \frac{\sqrt{I_{A,1} + I_{A,2} - I_{A,3} - I_{A,4}} \cdot \sqrt{3I_{A,2} - 3I_{A,3} - I_{A,1} + I_{A,4}}}{I_{A,2} + I_{A,3} - I_{A,1} - I_{A,4}} \tag{7.10}$$

For the second state also 4 phase shifted interferograms are recorded:

$$
\begin{aligned}
I_{B,1} &= a_R{}^2 + a_O{}^2 + 2a_R a_O \cos(\varphi_0 - \varphi_R + \Delta\varphi) \\
I_{B,2} &= a_R{}^2 + a_O{}^2 + 2a_R a_O \cos(\varphi_0 - \varphi_R + \Delta\varphi + \alpha) \\
I_{B,3} &= a_R{}^2 + a_O{}^2 + 2a_R a_O \cos(\varphi_0 - \varphi_R + \Delta\varphi + 2\alpha) \\
I_{B,4} &= a_R{}^2 + a_O{}^2 + 2a_R a_O \cos(\varphi_0 - \varphi_R + \Delta\varphi + 3\alpha)
\end{aligned}
\tag{7.11}
$$

The solution is:

$$
\begin{aligned}
&\varphi_O - \varphi_R + \Delta\varphi \\
&= \arctan \frac{\sqrt{I_{B,1} + I_{B,2} - I_{B,3} - I_{B,4}} \cdot \sqrt{3I_{B,2} - 3I_{B,3} - I_{B,1} + I_{B,4}}}{I_{B,2} + I_{B,3} - I_{B,1} - I_{b,4}}
\end{aligned}
\tag{7.12}
$$

The interference phase $\Delta\varphi$ is now calculated from Eq. (7.10) and (7.12) by subtraction.

Phase shifting speckle interferometry is sometimes also called *Electro-Optic Holography* (EOH).

7.2 Digital Shearography

ESPI as well as conventional and Digital HI are very high sensitive to optical path changes. Displacement measurements with a resolution of up to one hundredth of the wavelength are possible. On the other hand this high sensitivity is also a drawback for applications in a rough environment, where no vibration isolation is available. Unwanted optical path length variations due to vibrations disturb the recording process.

Shearography [8, 51, 52, 82, 108] is an interferometric method, which brings the rays scattered from one point of the object $P(x, y)$ into interference with those from a neighbouring point $P(x + \Delta x, y)$. The distance between both points is Δx. The shearing can be realized e. g. by a glass wedge, mounted in one half of the imaging system, figure 7.4. The object is imaged via both halfes of the aperture (with and without wedge). Therefore two laterally sheared images overlap at the recording device, see figure 7.5.

The intensity on the target is:

$$
\begin{aligned}
I_A(x, y) &= \left| a_1(x, y) \exp(i\varphi(x, y)) + a_2(x, y) \exp(i\varphi(x + \Delta x, y)) \right|^2 \\
&= a_1{}^2 + a_2{}^2 + 2a_1 a_2 \cos(\varphi(x, y) - \varphi(x + \Delta x, y))
\end{aligned}
\tag{7.13}
$$

where $a_1 \exp(i\varphi(x, y))$ and $a_2 \exp(i\varphi(x + \Delta x, y))$ are the complex amplitudes of the interfering waves in the image plane. As for ESPI the phase difference $(\varphi(x + \Delta x, y) - \varphi(x, y))$ varies randomly from point to point. This speckle inter-

ferogram is recorded and electronically stored. Another interferogram is recorded for the second state B:

$$
\begin{aligned}
& I_B(x,y) \\
& = \left| \begin{aligned} & a_1(x,y)\exp\left[i\left(\varphi(x,y)+\Delta\varphi(x,y)\right)\right] \\ & + a_2(x,y)\exp\left[i\left(\varphi(x+\Delta x,y)+\Delta\varphi(x+\Delta x,y)\right)\right] \end{aligned} \right|^2 \\
& = {a_1}^2 + {a_2}^2 \\
& + 2a_1a_2\cos\left[\varphi(x,y)-\varphi(x+\Delta x,y)+\Delta\varphi(x,y)-\Delta\varphi(x+\Delta x,y)\right]
\end{aligned}
\tag{7.14}
$$

Pointwise subtraction gives:

$$
\begin{aligned}
& \Delta I = \left| I_A - I_B \right| \\
& = \left| 2a_1a_2 \left\{ \cos\left(\varphi(x,y)-\varphi(x+\Delta x,y)\right) - \cos\left[\begin{aligned} & \varphi(x,y)-\varphi(x+\Delta x,y) \\ & +\Delta\varphi(x,y)-\Delta\varphi(x+\Delta x,y) \end{aligned} \right] \right\} \right| \\
& = 2a_1a_2 \left| \begin{aligned} & \sin\left\{ \varphi(x,y)-\varphi(x+\Delta x,y)+\frac{\Delta\varphi(x,y)-\Delta\varphi(x+\Delta x,y)}{2} \right\} \\ & \times \sin\frac{\Delta\varphi(x,y)-\Delta\varphi(x+\Delta x,y)}{2} \end{aligned} \right|
\end{aligned}
\tag{7.15}
$$

This correlation pattern is named *shearogram*, see typical example in figure 7.6.

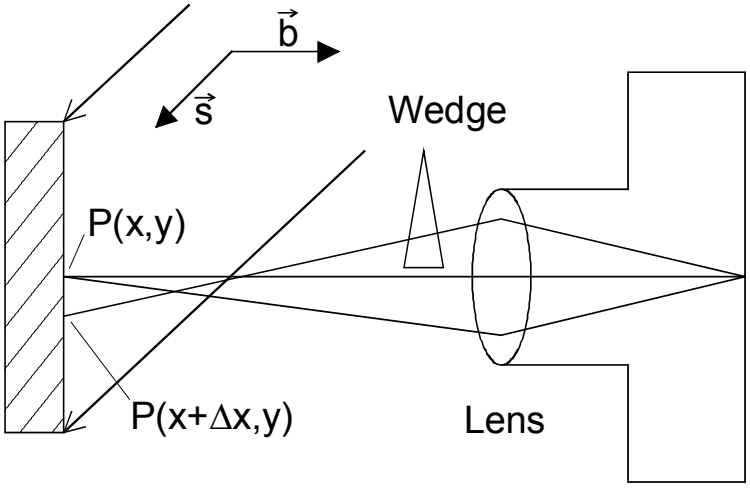

Fig. 7.4. Speckle shearing interferometer

Fig. 7.5. Image of a shearing camera

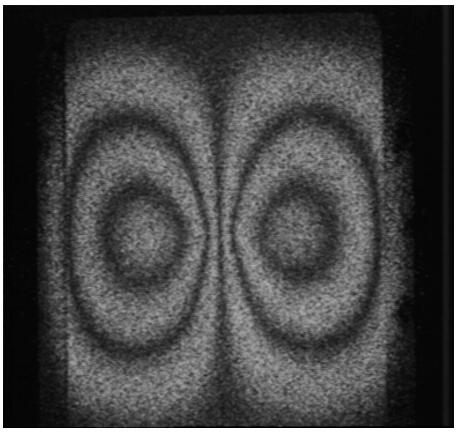

Fig. 7.6. Shearogram

The phase shift due to deformation in the argument of Eq. (7.15) is calculated as follows (see also the definition of unit vectors $\vec{b}$ and $\vec{s}$ in figure 7.4):

$$\begin{aligned}
&\Delta\varphi(x,y)-\Delta\varphi(x+\Delta x,y) \qquad (7.16)\\
&=\frac{2\pi}{\lambda}\left\{\vec{d}(x,y)\left(\vec{b}-\vec{s}\right)-\vec{d}(x+\Delta x,y)\left(\vec{b}-\vec{s}\right)\right\}\\
&=\frac{2\pi}{\lambda}\left\{\frac{\vec{d}(x,y)-\vec{d}(x+\Delta x,y)}{\Delta x}\left(\vec{b}-\vec{s}\right)\right\}\Delta x\\
&\approx\frac{2\pi}{\lambda}\frac{\partial\vec{d}(x,y)}{\partial x}\left(\vec{b}-\vec{s}\right)\Delta x
\end{aligned}$$

A shearing interferometer is therefore sensitive to the derivative of the displacement into the shear direction, in contrast to ESPI which is sensitive to the displacement. Shearography is relatively insensitive for rigid body motions, because $\partial\vec{d}(x,y)/\partial x$ vanishes if the object is moved as a whole [149, 150]. A second property which makes a shearing interferometer less sensitive to vibrations is the self-reference principle: Optical path changes due to vibrations influence both partial beams, which means they compensate each other to a certain degree. Shearography is therefore suited for rough environments with low vibration isolation.

The measurement sensitivity of a speckle shearing interferometer can be adjusted by varying the shearing Δx. This parameter is determined by the wedge angle in the interferometer set-up of figure 7.4. Other shearing interferometer geometries are based on a Michelson interferometer, where the mirror tilt determines the shearing, figure 7.7.

The phase shifting techniques can be used also for shearography. As for ESPI a set of phased shifted images is recorded in each state from which the phase according to Eq. (7.16) is calculated.

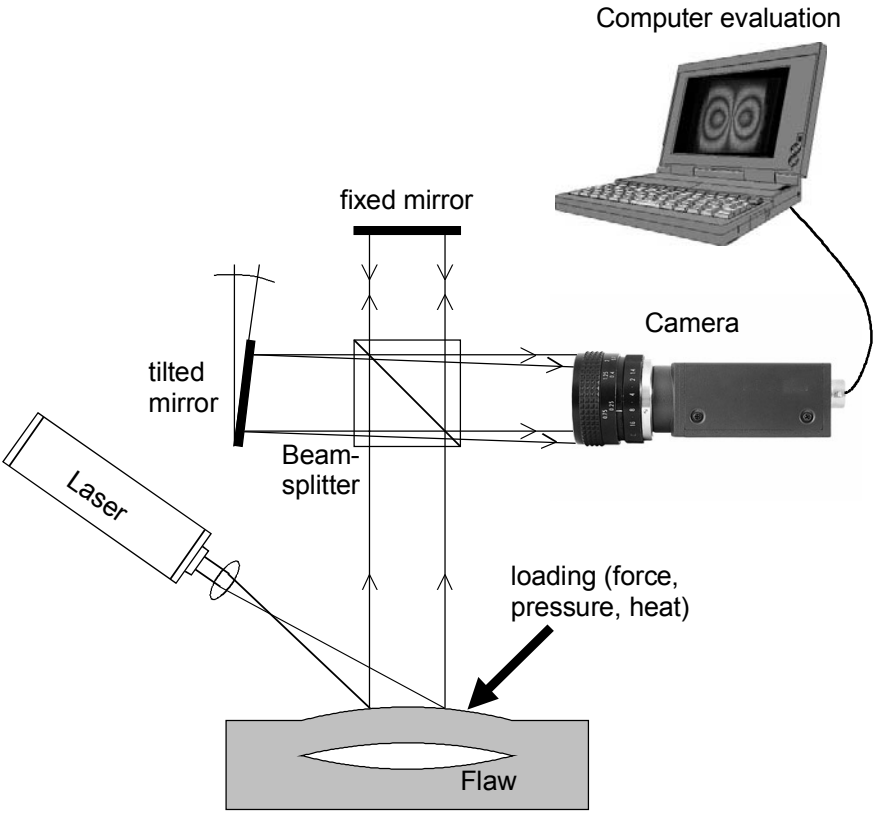

Fig. 7.7. Shearography set-up based on a Michelson interferometer

7.3 Digital Speckle Photography

Digital Speckle Photography (DSP) is the electronic version of Speckle Photography [15, 50, 83, 145, 154]. The method is used to measure in-plane displacements and strains. In classical Speckle Photography two speckle patterns of the same surface are recorded on photographic film, e. g. with the set-up of figure 2.9. The object suffers an in-plane deformation between the exposures. This in-plane deformation is made visible as fringe pattern by pointwise illumination of the double exposed film with a collimated laser beam or alternatively using an optical filtering set-up. In DSP the speckle patterns are recorded by a high resolution CCD-camera, electronically stored and correlated numerically. DSP has the potential to measure under dynamic testing conditions, because a single recording at each load state is sufficient for the evaluation. Furthermore, the requirements for vibration isolation are much lower than for interferometric methods, because DSP works without reference wave. DSP is therefore an attractive tool for measurements under workshop conditions.

The sample under investigation is coherently illuminated by means of an expanded laser beam. A speckle pattern of the reference state and a speckle pattern of the load state are recorded. The first step of the numerical evaluation procedure is to divide the whole image of e. g. 2024 × 2024 pixels into subimages, figure 7.8. Usual sizes of these subimages are 64 × 64 pixels or 32 × 32 pixels. The calculation of the local displacement vectors at each subimage is performed by a cross correlation function

$$R_{II}(d_x, d_y) = \int_{-\infty}^{\infty}\int_{-\infty}^{\infty} I_1^*(x,y) I_2(x+d_x, y+d_y)\,dx\,dy \tag{7.17}$$

where $I_1(x,y)$ and $I_2(x,y)$ are the intensities in the reference and in the load speckle pattern, respectively. The quantities d_x and d_y are the displacements of the subimage in *x*- and *y*-direction. Intensities are always real, i. e. the conjugate complex operation can be neglected. A mathematical equivalent form of Eq. (7.17) is:

$$R_{II}(d_x, d_y) = \Im^{-1}\left\{\Im\left[I_1^*(x,y)\right]\Im\left[I_2(x,y)\right]\right\} \tag{7.18}$$

The mean displacement vector of the evaluated subimage is given by the location of the peak of the cross correlation function, figure 7.8. This numerical evaluation corresponds to the classical technique, where double exposed speckle photos are locally illuminated by a collimated laser beam. The full in-plane displacement map of the monitored area is available after evaluation of all subimages.

The displacement field is calculated by this methods in integer numbers of one pixel. The accuracy is therefore only in the order of one pixel. This discrete evaluation is sufficient for applications where only displacements fields are to be measured. Strain analyses of experimental mechanics require often a higher meas-

urement accuracy, because differences have to be calculated. The normal strains are e. g. given by

$$\varepsilon_x = \frac{\partial d_x}{\partial x} \approx \frac{\Delta d_x}{\Delta x} \quad ; \quad \varepsilon_y = \frac{\partial d_y}{\partial y} \approx \frac{\Delta d_y}{\Delta y} \tag{7.19}$$

The accuracy of DSP can be improved using so called subpixel algorithms, where the displacements are calculated on the basis of all floating point values in the neighborhood of the pixel with the peak location. A simple subpixel algorithm is given by

$$d_x = \frac{\sum_i d_{x,i} G_i}{\sum_i G_i} \quad d_y = \frac{\sum_i d_{y,i} G_i}{\sum_i G_i} \tag{7.20}$$

where G_i is the floating point grey level of pixel number i. The structure of this formula is equivalent to a "center of gravity" calculation. In practice only a few pixels around the peak are necessary for the subpixel evaluation.

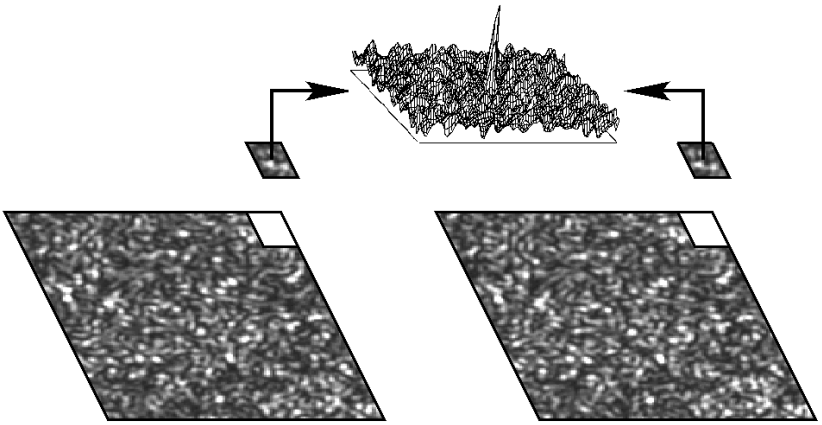

Fig. 7.8. Cross correlation of subimages

7.4 Comparison of Conventional HI, ESPI and Digital HI

Conventional Holographic Interferometry using photographic or other recording media, Electronic Speckle Pattern Interferometry and Digital Holographic Interferometry are different methods to measure optical path changes. In this chapter the differences as well as the common features of all three methods are analyzed.

The process flow diagram of conventional real-time HI is shown in figure 7.9. The measurement process starts by recording of a hologram of the object in its initial state. This is the most time-consuming and costly step of the entire process:

The exposure, development and repositioning of a photographic plate takes typically some minutes. Other holographic recording media such as thermoplastic films or photorefractive crystals can be developed much faster and automated (some seconds for thermoplastic films, even instantaneously for photorefractive crystals). However, the quality and reliability of thermoplastic films is not sufficient for HI applications and the information stored in photorefractive crystals erases in the optical reconstruction process. Once the hologram is successfully developed and replaced at its initial position the process is simple: The superposition of the wave field reconstructed by the hologram with the actual wave field generates a holographic interferogram. This fringe pattern is recorded by an electronic camera and digitally stored. In order to determine the interference phase unambiguously, it is necessary to generate at least three interferograms (for the same object state) with mutual phase shifts. The interference phase is calculated from these phase shifted interferograms by the algorithm briefly discussed in chapter 2.7.5. The entire process requires altogether the generation of one hologram plus recording of at least three interferograms in order to determine the interference phase. The technical effort is tremendous: A holographic set-up with interferometer and laser, holographic recording media (photographic plates), laboratory equipment for development of holograms, a phase shifting unit and an electronic camera with storage device (PC) for interferogram recording are necessary. On the other hand the quality of interferograms generated by this method is excellent. Due to the size and resolution of holograms recorded on photographic plates the observer can choose the observation direction freely, i. e. it is possible to observe the object from a variety of different positions and with different depth of focus. This is often very helpful for NDT applications and, if the sensitivity vector has to be varied, in quantitative deformation measurement.

ESPI was born from the desire to replace photographic hologram recording and processing by recording with electronic cameras. At the beginning of the seventieth of the last century, when ESPI was invented, only analogous cameras with very low resolution (linepairs per millimetre) were available. Consequently, a direct conversion of holographic principles to electronic recording devices was not possible. The basic idea of ESPI therefore was to record holograms of focussed images. The spatial frequencies of these image plane holograms could be adapted to the resolution of the cameras due to the in-line configuration. The optical reconstruction was replaced by an image correlation (subtraction). The ESPI correlation patterns have some similarities to the fringes of HI, but have a speckle appearance. Another difference to conventional HI is the loss of the 3D-effect, because only image plane holograms are recorded from one observation direction. Interference phase measurement with ESPI require application of phase shifting methods, see process flow in figure 7.10. In each state at least three speckle interferograms with mutual phase shifts have to be recorded. The total number of electronic recordings to determine the interference phase is therefore at least six. Speckle interferometers are commercially available. These devices can be used nearly as simple as ordinary cameras.

The idea of Digital Holographic Interferometry was to record "real" holograms (not holograms of focussed images) by an electronic device and to transfer the op-

tical reconstruction process into the computer. The method is characterized by following features:

- No wet-chemical or other processing of holograms (as for ESPI)
- From one digital hologram different object planes can be reconstructed by numerical methods (numerical focussing)
- Lensless imaging, i. e. no aberrations by imaging devices
- Direct phase reconstruction, i. e. phase differences can be calculated directly from holograms, without interferogram generation and processing. This interesting feature is only possible in DHI, conventional HI as well as ESPI need phase shifted interferograms (or another additional information) for phase determination. The total number of recordings to get the interference phase is therefore only two (one per state), see process flow in figure 7.11. Even transient processes, where there is no time for recording of phase shifted interferograms, can be investigated with DHI.

DHI and phase shifting ESPI are competing techniques. ESPI is working since many years in real-time, i. e. the recording speed is only limited by the frame rate of the recording device (CCD). In addition the user sees directly an image of the object under investigation, while this image is only available in DHI after running the reconstruction algorithm. This *what you see is what you get* feature is helpful for adjustment and control purposes. On the other hand the time for running the DHI reconstruction algorithms has been reduced drastically in recent years due to the progress in computer technology. Digital holograms with 1000×1000 pixels can nowadays be reconstructed also nearly in real-time.

Another slight *present* disadvantage of DHI is that the spatial frequency spectrum has to be adapted carefully to the resolution (pixel size) of the CCD. However, also the CCD technique makes progress and CCD's with further decreasing pixel distances may be expected in future, allowing a greater object angle cone.

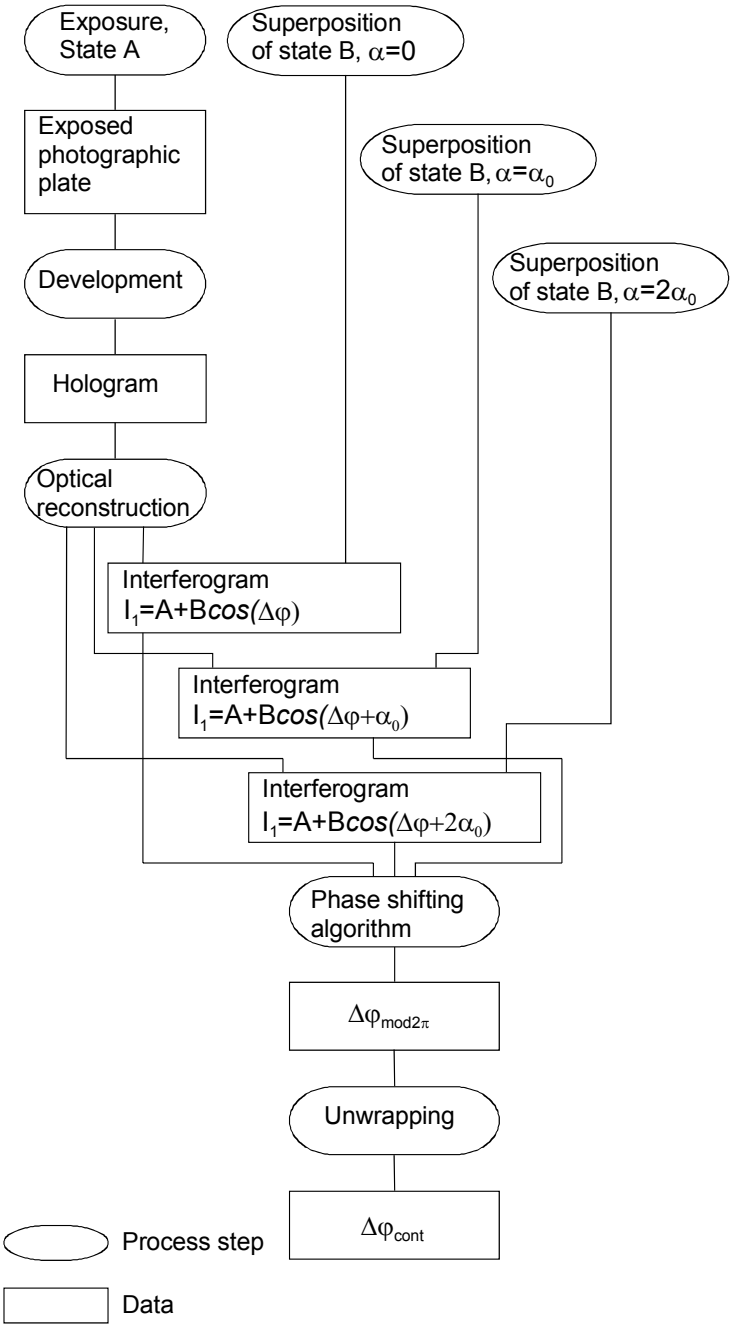

Fig. 7.9. Process flow of real-time HI with phase shifting fringe evaluation

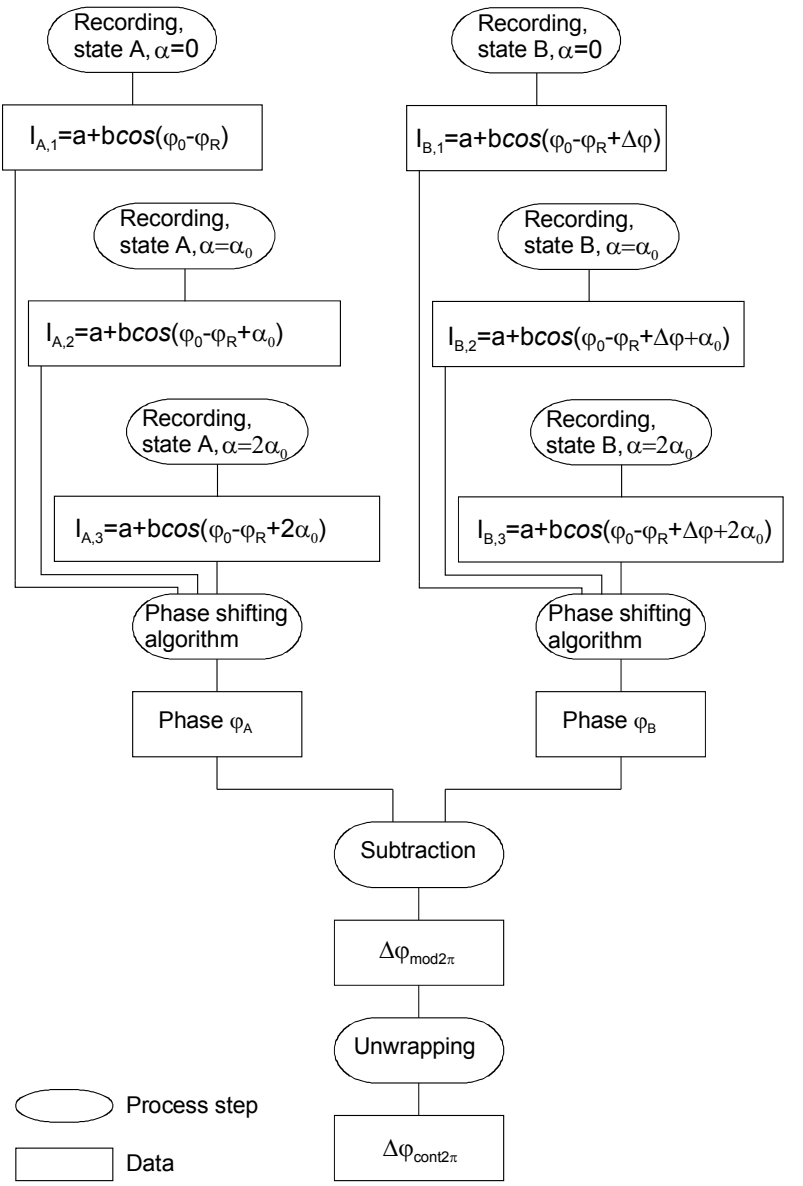

Fig. 7.10. Process flow of phase shifting ESPI

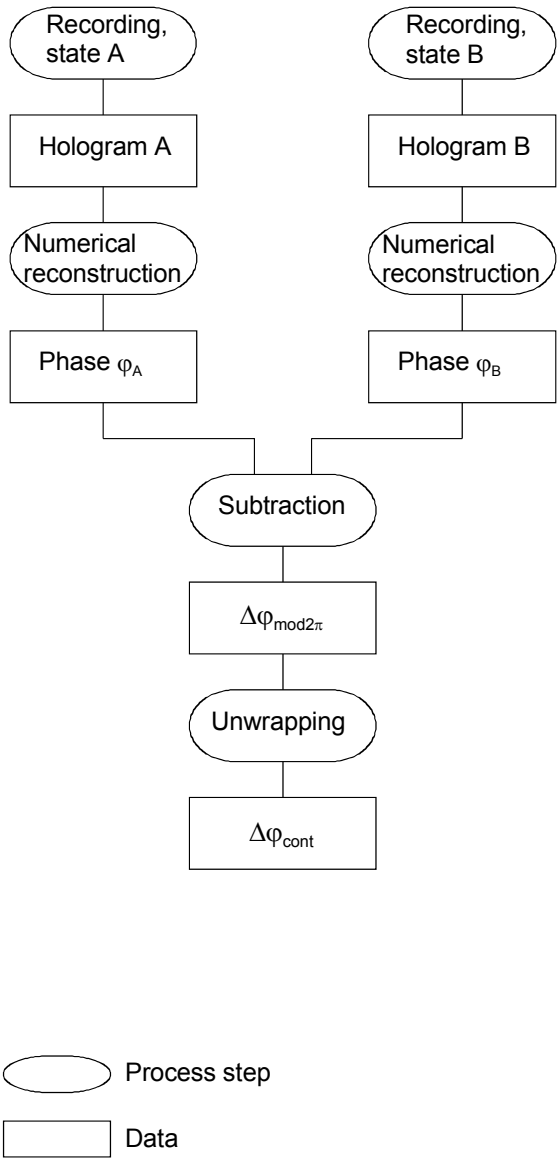

Fig. 7.11. Process flow of Digital HI